J Nanostruct 13(2): 325-340, Spring 2023

RESEARCH PAPER

Improvement of Neurite Outgrowth in PC12 Cells by TiO_2, Au/TiO_2 and Ag/TiO_2 Nanoparticles

Samaneh Katebi Koushali [1], *Masood Hamadanian* [1,2] *

[1] *Department of Physical Chemistry, Faculty of Chemistry, University of Kashan, Kashan, I.R. Iran*

[2] *Institute of Nanoscience and Nanotechnology, University of Kashan, Kashan, I.R. Iran*

ARTICLE INFO

Article History:
Received 10 January 2023
Accepted 25 March 2023
Published 01 April 2023

Keywords:
Differentiation
Nerve growth factor
PC12 cells
TiO_2 nanoparticle

ABSTRACT

There are numerous applications of nanomaterials in catalysis, biosensing, biotechnology, electronics, magnetic fluids, energy storage and also in the biomedical field, especially in gene or drug delivery and diagnostics. Nanomaterials have amazing capabilities to stimulate neuronal cells toward neuronal cell proliferation, neuronal cell adhesion, axonal growth, and neuroprotection. Researchers have demonstrated that nanomaterials can also differentiate stem cells into neuronal cells. Recently, the impact of nanomaterials on the proliferation and differentiation of normal, cancer, and stem cells have been investigated greatly. In this study, the effects of titanium dioxide nanoparticles (TiO_2NPs) on the differentiation of neural stem cells are examined. Our findings indicate that TiO_2 nanoparticles lead to differentiation tendencies biased towards neurons from neural stem cells, suggesting TiO_2 nanoparticles might be a beneficial inducer for neuronal differentiation. We found that pheochromocytoma cell line (PC12 cells) exposed to TiO_2, Au/TiO_2, Ag/TiO_2 nanoparticles significantly increased the differentiation of neural stem cells and promoted neurite outgrowth. Our data may have resulted from the stimulation of cell adhesion molecules that are associated with cell-matrix interactions through nanoparticle. The findings of this work proposes the use of the Ag/TiO_2 nanoparticles which also have antibacterial and antioxidant characteristics, as a suitable method to improve Nerve Growth Factor (NGF) activity and efficacy, thus, opening the novel window for substantial neuronal repair therapeutics.

How to cite this article
Katebi Koushali S, Hamadanian M . Improvement of Neurite Outgrowth in PC12 Cells by TiO_2, Au/TiO_2 and Ag/TiO_2 Nanoparticles. J Nanostruct, 2023; 13(2):325-340. DOI: 10.22052/JNS.2023.02.002

INTRODUCTION

Nanomaterials are considerably applied in cosmetic, textile, electronic, magnetic fluid, and pharmaceutical industries. Nevertheless, nanomaterials are potentially applied enormously to diagnose and treat a variety of illnesses because they possess specific physicochemical features, in particular antibacterial, antimicrobial, anti-inflammatory, and anticancer activities [1-4].

The retrieval of neural functions and

* *Corresponding Author Email: hamadani@kashanu.ac.ir*

restoration has been a subject of importance in neuroscience concerning the therapy of post-accident damaged neurons or a degenerative illness. Neural precursor cells are neural stem cells (NSCs) situated specifically in the central nervous system (CNS). NSCs are capable of self-renewal and multi-potential differentiation [5] being capable of differentiation into neurons or glial cells (microglial or astrocytes cells) [6, 7]). The neural cells that are newly differentiated may be able to substitute missing cells to improve diseases and functions of the nervous system [8] .This neurogenesis capability drastically helps in the treatment of some traumatized nervous tissues or neurodegenerative disorders, including Alzheimer's and Parkinson's disease.

Both neurobiological and neurotoxicological investigations frequently use pheochromocytoma cell lines (PC12 cells) as a model for differentiating neurons. NSCs differentiation into neurons or remaining in a proliferous condition is determined by the molecular mode of action, but this molecular procedure is not still well known. The differentiation of NSCs has been shown to be dependent on some special factors, but achieving a distinct outline of the differentiation phases remains difficult. To induce cell differentiation, growth factors (GFs) are the crucial factors [9]. More effective results and improved potential treatments can be achieved by enhancing the natural impact of GFs throughout the differentiation process. As a vital GF, Nerve Growth Factor (NGF) is essential for maintaining and developing neurons in the peripheral nervous system. The proliferation of spread-out neurites is stopped and undergoes electrical impulsivity by NGF-incubated PC12 cells. The differentiation process with NGF activates TrkA receptors that trigger several signaling routes, including the Ras-extracellular Signal-regulated Kinase (ERK) cascade and phosphatidylinositol 3-kinase (PI3K) pathway, encouraging neurite growth and hindering multiplication.

The exclusive and useful physical, chemical, and mechanical features of nanomaterials have led to their wide-ranging uses in the whole scientific fields, particularly biomedicine. Accordingly, the impact of nanoparticles (NPs) on the differentiation procedure of NSCs is interesting in research projects [10].

The last few years have witnessed extensive investigations on the response of nanomaterials to neural cells. The adhesion of neural cells to neural cells, neural cell multiplication, axonal growth, and neuroprotection are stimulated by the superb abilities of nanomaterials. The differentiation of stem cells into neural cells has also been proven by nanomaterials. The differing sizes, forms, and chemical compositions of nanomaterials, such as nanoparticles, nanofibers, nanotubes, nanocone, and nanoemulsion, generally created stimulating impacts on neural cells, however, some of them exert inhibitive impacts on neural cells. For instance, neuronal growth, neuroprotection, and neural renewal were promoted by nanofibers and nanotubes, which also activated the functions of hippocampal neurons. Additionally, nanocomplexes, nanomembrane, and nanoscaffold in neuronal tissue reconstruction and neuronal renewal are reportedly used in some studies [9-11].

In recent years, the impacts of diverse NPs on neurons have been studied in various investigations. As reported frequently, NPs are suggested to stimulate neural differentiation and neuroprotection studied both in vivo and in vitro [12-17]. Better therapeutical outcomes have been obtained by examining various groups of NPs, among which carbon-based NPs are widely observed in reports, [18-23] followed by silver and gold NPs [24-26].

Wide-ranging biomedical applications use metallic and metal oxide NPs, which is attributable to their exclusive physical and chemical features. Some of these properties include high surface energy, a high surface area to volume ratio, high energy atoms positioned on the particle surface area, [27] surface plasmon resonances (SPR), existence of edges and corners, and high dangling band and electron storage energy [28, 29].

Various shapes and sizes of metallic and metal oxide NPs are obtainable with diverse techniques, such as physical, chemical, and biological procedures. Pure metallic NPs are represented by Gold (Au), Copper (Cu), and Silver (Ag), whereas Titanium dioxide (TiO_2), Iron oxide, Zinc oxide, Cerium oxide (nanoceria), and Silicate (SiO_2) are metal oxide NPs with good reputations for their application in biomedicine and pharmacology [30].

The exclusive features, little toxic effects, and biocompatible properties have made Au NPs promising substances to direct the fate of stem cells and tissue renewal. The differentiation of mouse ESCs (mESCs) into dopaminergic (DA) neurons was stimulated by Au NPs, which was

caused by activating the mTOR/p70S6K signaling route promoted by Au NPs [24]. Elongated axons and increased neurite length were obtained by the nanocomposite of Au NPs [31]. Ag NPs measuring 10-20 nm [32] and 30 nm [33] exerted no noticeable toxicity on the differentiation of mesenchymal stem cells (MSCs) [34]. There are investigations regarding the impacts of Ag NPs on differentiation of stem cells [35].

TiO_2 falls into the leading biomaterials as it shows good cytocompatibility and bioactivity, and TiO_2-based materials with various sizes and morphologic features are synthesized by several techniques for various applied fields [36, 37]. The exclusive chemical and mechanical specifications and the biocompatible property of Ti have made it a reputed material in prosthetics and dental applications [38, 39]. The impact of TiO_2 NPs on the stimulation of the neural differentiation of mNSCs was accentuated in a study based on protein interaction network analysis. To validate this analysis, a positively expressed neuronal marker, ßIII-tubulin, was shown using immunofluorescent staining and fluorescence-activated cell sorting (FACS) analyses [40].

Additionally, some investigators have discovered that TiO_2 NPs or nanotubes positively influence the behavior of bone MSCs [41, 42]. The adipogenic differentiation of rBM-MSCs was not negatively affected by TiO_2–COOH, TiO_2–NH_2, and TiO_2–PEG [43]. The stimulated osteogenic differentiation of hBM-MSCs cultures on the TiO_2 surface was compared with cells cultured on a coverglass [44]. Furthermore, cells grown on the TiO_2 surface presented elevated attachment, mediating the phosphorylation of Focal Adhesion Kinase (FAK) at a high level. The present research focuses on designing and preparing three types of TiO_2 NPs, i.e., a pure TiO_2 NP, and the other two types Au/TiO_2 and Ag/TiO_2 NPs. The impacts of these NPs were examined on the neurite outgrowth throughout differentiation. The neural differentiation model was designed using PC12 cells.

MATERIALS AND METHODS

Materials

Titanium tetraisopropoxide (TTIP), Glacial acetic acid, Ethanol (EeOH), Analytical grade methanol (MeOH), Silver nitrate ($AgNO_3$) and gold (III) chloride trihydrate ($HAuCl_4 \cdot 3H_2O$) were acquired from Merck. MTT (sodium 2, 3,-bis (2-methoxy-4-nitro-5-solfophenyl)-5-[(phenylamino)-carbonyl1]-2H-tetrazolium inner salt), Poly-L-ornithine (MW >300000) and dimethyl sulfoxide (DMSO) were purchased from Sigma, USA. K_2HPO_4 and KH_2PO_4 (acquired from Merck) were used to prepare phosphate buffer solution (PBS, 0.05 M, pH 7). NGF-ß (GFM 11) were obtained from cell guidance systems, USA. Bovine serum albumin (BSA), Fetal bovine serum (FBS), Horse serum (HS), L-glutamine, Penicillin- streptomycin and RPMI Medium were purchased from Gibco, USA. All solutions were made with double distilled water.

Preparation of TiO_2, Ag/TiO_2, Au/TiO_2 Nanoparticles

TiO_2, Au/TiO_2 (1%) and Ag/TiO_2 (1%) nanoparticles were prepared by sol–gel and photochemical method using TTIP, ethanol, glacial acetic acid, silver nitrate and gold (III) chloride trihydrate as precursors. To prepare TiO_2 nanoparticles, first, 4.65 mL of titanium tetraisopropoxide was hydrolyzed using glacial acetic acid (8.95 mL) at 0 °C. Then, deionized water (98.75 mL) was added drop wise under vigorous stirring for 2 h. Subsequently, the solution ultrasonicated for 20 min in ice bath and the stirring was continued for another 4 h and the solution ultrasonicated for 20 min in ice bath until a clear solution was formed. Afterwards, the prepared solution was kept in dark for nucleation process for 24 h. The solution was gelated in an oven at 80 °C for 12 h afterwards. The gel was dried at 120 °C and subsequently, the prepared powder was crushed well and calcined in the muffle furnace at 550 °C for 2 h.

To prepare Au/TiO_2 and Ag/TiO_2 nanoparticles, specific amounts of gold (III) chloride trihydrate (1%) and silver nitrate (1%) along with 0.4 g TiO_2 nanoparticles were added to 100 mL of deionized water and the solution was purged with high-purity N_2 atmosphere during vigorous stirring. Time of purgation depends on the volume of the deionized water and the imported gas. Then, the resulting solution was transferred to a quartz photocatalytic reactor and its head was covered and was put under UV irradiation for 12 h, during stirring. After this, the precursor was separated by centrifugation and was washed with deionized water for several times. The wet samples were dried at 110 °C for 12 h. Since photochemical deposition method is fast and inexpensive, therefore, it is a promising way to form noble metal-semiconductor nanocomposites in situ by reducing noble metal ions adsorbed on

the semiconductor surface.

Cell culture

PC12 cells were cultured in the RPMI medium supplemented with 5% fetal bovine serum (FBS), 10% horse serum (HS), 1% penicillin-streptomycin and 1% L-glutamine in a humidified incubator at 37 °C containing 5% CO_2. For differentiation, PC12 cells (5000 cells/cm^2) were seeded on PLO-laminin coated plates and incubated for 24 hours in serum-reduced media (0.5% FBS - 1% HS). Recombinant mouse NGF-β (Sigma-Aldrich, USA) was added to the medium (every two days) to induce the differentiation of PC12 cells. Then, five treatments were examined: Control (free NGF), 50 ng/ml-NGF, NGF-TiO_2 nanoparticles (20µg/ml), NGF-Au/TiO_2 nanoparticles (20µg/ml), and NGF-Ag/TiO_2 nanoparticles (20µg/ml).

Measurement of neurite outgrowth of PC12 cells

Neurite outgrowth of PC12 cells was studied in this work. PC12 cells were incubated with NGF and different synthesized nanoparticles (TiO_2, Au/TiO_2 and Ag/TiO_2). After incubation, the percentage of neurite outgrowth and the number of branching points were quantified.

The effect of different treatments on neuronal differentiation

In this study, TiO_2, Au/TiO_2 and Ag/TiO_2 nanoparticles with a size of 23-29 nm were used. First, the efficiency of free NGF as a differentiating factor was measured. Based on the results PC12 cells treated with free NGF demonstrated neurite outgrowth and the development of a complex neuronal network signifying that NGF was active. The efficiency of free NGF treatment was compared to other treatments such as pure TiO_2 nanoparticles and using Au and Ag in the surface of TiO_2 nanoparticles. The PC12 (2×10^3) cells were plated on PLO coated plates and incubated with five deferent treatments. Part 1 (tree wells), was kept as the control sample. Part 2, was mixed with free NGF alone. Part 3 was mixed with NGF (50 ng/ml) and pure TiO_2 nanoparticles (20 µg/ml). Part 4, was incubated with NGF and Au/TiO_2 nanoparticles (20 µg/ml) and Part 5 was incubated with NGF and Ag/TiO_2 nanoparticles (20µg/ml). After incubation in different treatments, PC12 cells were washed and fixed with 4% paraformaldehyde for 30 min. Percentage of branching points, neurite outgrowth and differentiation of PC12 cells under different treatments were measured using the light microscope.

Cresyl Violet Staining (Nissl Staining)

PC12 cells were stained with 0.1% Cresyl Violet solution for 4-15 min and washed 3 times with PBS to remove excess stain. PC12 cells were photographed through inverted microscopy and scored for the presence of Nissl substance (rough endoplasmic reticulum) and neurites.

Immunofluorescence staining

PC12 cells were immunostained with anti-b3-tubulin, which is an important neural specific marker to visualize the neurites in PC12 cells during differentiation. PC12 cells were treated with different TiO_2 nanoparticles and were fixed with 4% paraformaldehyde for 30 min. Afterwards, permeabilized with 0.3% Triton X-100 diluted in PBS. PC12 cells were incubated with a β3-tubulin monoclonal antibody, which was diluted to 1:300 in 1% BSA blocking buffer (PBS with 0.2% Tween 20) for 2 h and washed 3 times with PBS. The cells were then incubated with a FITC-conjugated secondary antibody, which was diluted to 1:300 in 2% BSA blocking buffer, for 1 h. Nuclei was marked with DAPI (blue) for 15 min. Fluorescent images were taken using the fluorescence microscopy.

Cell viability assay

The MTT assay was tested to investigate the cytotoxic effects of TiO_2, Au/TiO_2 and Ag/TiO_2 nanoparticles on PC12 cells. 10000 cells were seeded onto the PLO - coated 96-well plates. 24 h after incubation, PC12 were treated with different TiO_2 nanoparticles at concentrations ranging from 5 to 100 µg/ml. PC12 cells were incubated with 0.5 mg/ml MTT according to the Mosmann method. Absorbance was measured using the ELISA reader at 560 nm.

Statistical analysis

Error bars represent standard deviations. The analysis method was a one-way ANOVA followed by a Scheffé Post-Hoc as a multiple comparison test (SPSS software version 20.0, SPSS Inc). A p value of 0.05 was considered statistically significant.

Instrumentation

The morphology of the TiO_2, Au/-TiO_2 and Ag/TiO_2 nanoparticles were analyzed by Scanning Electron Microscopy (SEM, model S-4160, Hitachi, Japan) and Energy-Dispersive X-ray spectroscopy

(EDX) analysis (Peronis 2100, Japan). The crystal phase of the synthesized nanoparticles were detected by X-ray diffraction (XRD) patterns (Philips X'pert pro MPD model X-ray diffractometer using Cu Kα radiation as the X-ray source, USA). FT-IR spectra of the nanoparticles were registered by the Fourier transform infrared (FT-IR) spectrometer (Nicolet Magna IR 550, USA). UV–vis absorption spectra of the synthesized nanoparticles were obtained with a UV–vis diffuse reflectance spectroscopy (DRS) (Shimadzu, model UV-1800, Japan). A light microscope (Inverted Microscope Diaphot-TMD; Nikon, Tokyo, Japan) 10x-40x objective lens and a digital camera (Coolpix 990; Nikon) was used to capture the images with the manual setting. Fluorescent images were taken

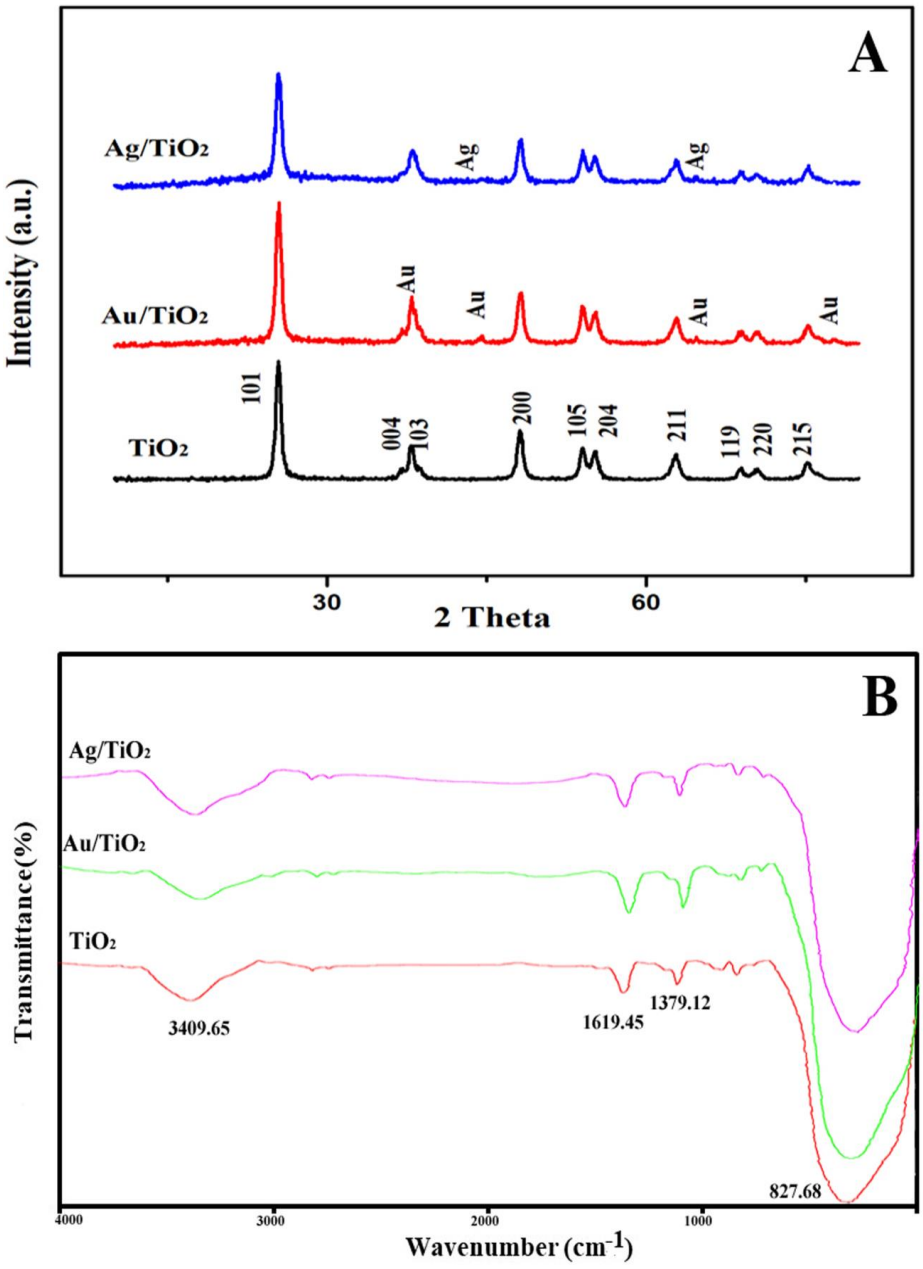

Fig. 1. XRD patterns (A) and FT-IR spectrum (B) of TiO_2, Au/TiO_2 and Ag/TiO_2 nanoparticles.

using the fluorescence microscopy (Olympus IX71, Japan). Absorbance was measured using the ELISA reader (Thermo LabSystems, USA).

Results AND DISCUSSION

Crystalline structure

The crystal structure of our synthesized samples (TiO_2, Au/ TiO_2 and Ag/TiO_2 nanoparticles) was examined by X-ray diffraction (XRD) analysis. As is shown in Fig. 1A, a typical pattern for TiO_2 nanoparticles was observed and the structure was confirmed based on the Joint Committee on Powder Diffraction Standards (JCPDS) Card file No. 00-001-0562. The crystalline peaks with 2θ

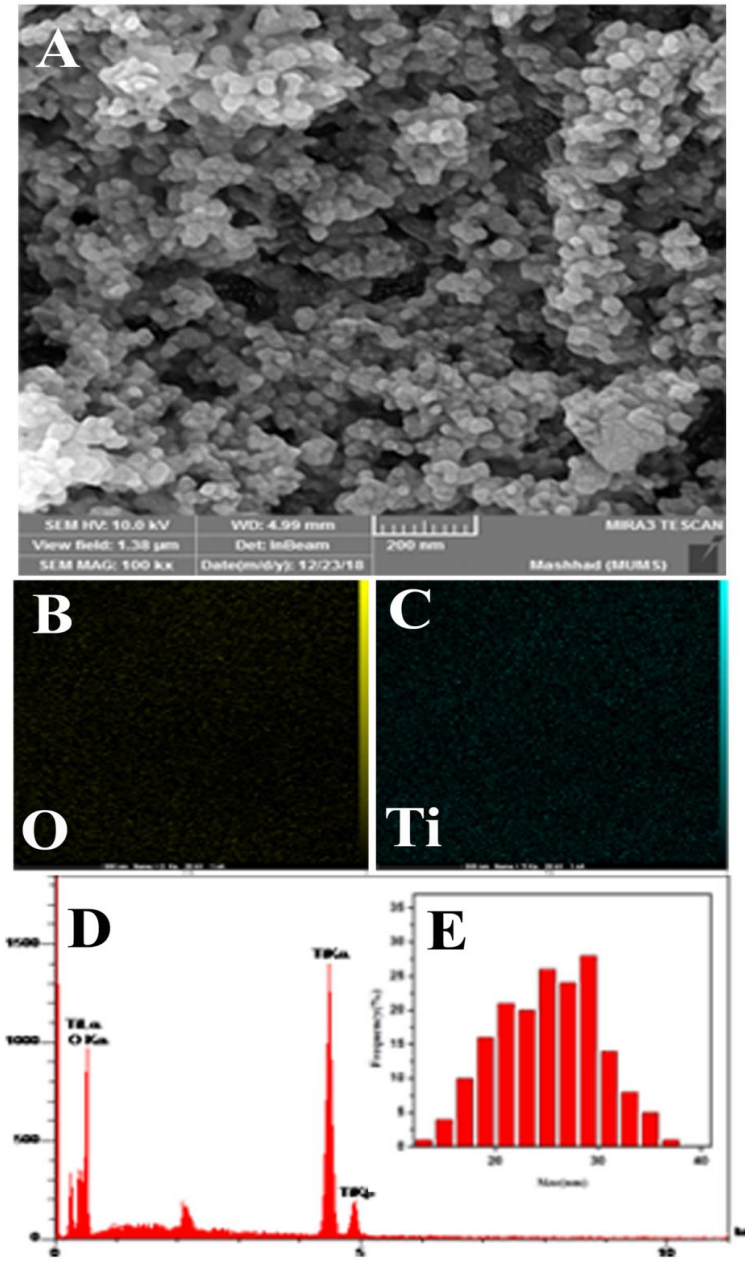

Fig. 2. SEM-EDS analysis results of TiO_2 NPs: (A) SEM image (B)–(C) EDS mapping result from (A) a SEM image showing the distribution of (B) O and (C) Ti in a mass of TiO_2 NPs. (D) EDS spectrum (E) the corresponding particle size distributions.

values of 25.21°, 37.76°, 48.02°, 54.05°, 55.03°, 62.80°, 68.85°, 70.19°, and 75.07° can be exactly indexed to the tetragonal anatase structured TiO_2. The sharp diffraction peaks indicate the good crystallinity of the synthesized TiO_2 nanoparticles and no peaks for rutile and brookite structures are detected in the spectra. Furthermore, negligible and diffraction peaks that are attributed to Au and Ag could be observed and the structure was confirmed based on the (JCPDS) Card file No. 01-076-1489 and 00-001-1172 respectively. However, the diffraction peaks of Au and Ag did not appear

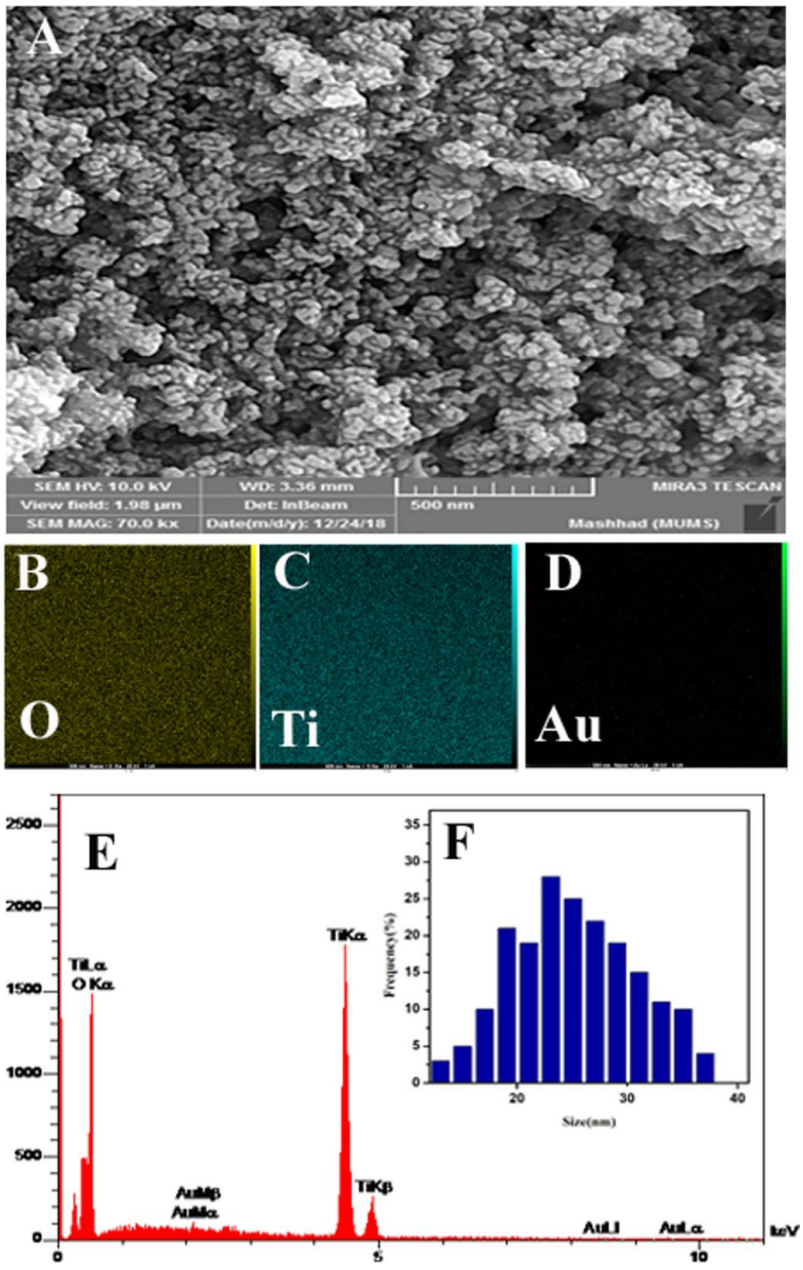

Fig. 3. SEM-EDS analysis results of Au/TiO_2 NPs: (A) SEM image (B)–(D) EDS mapping result from (A) a SEM image showing the distribution of (B) O, (C) Ti and (D) Au in a mass of Au/TiO_2 NPs. (E) EDS spectrum (F) the corresponding particle size distributions.

well in this pattern, suggesting that the amount of Au and Ag were too low to be detected by XRD. It can be seen that the XRD curve of Au/TiO_2 exhibits evident diffraction peaks at 38.2º, 44.4º, 64.6º and 77.6º which could be indexed well to the (111), (200), (220), (311) facets of the typical fcc phase of Au, respectively. In the XRD pattern of Ag/TiO_2 samples, the Ag metallic peak was shown at 44.4 º, and one more weak Ag metallic peak occurred at 64.5º. These patterns confirmed the crystallinity of the particles. The crystallite size can be estimated from the widths of the X-ray diffraction peaks (the most intense peaks for each sample) using Scherrer's equation. Inserting the experimental data for a pronounced peak: $2\theta=25.45^{\circ}$, the average crystallite size of TiO_2, Au/TiO_2 and Ag/TiO_2 was measured (d=29, 23 and 25nm respectively). Doping metal ions in TiO_2 has been proven to be

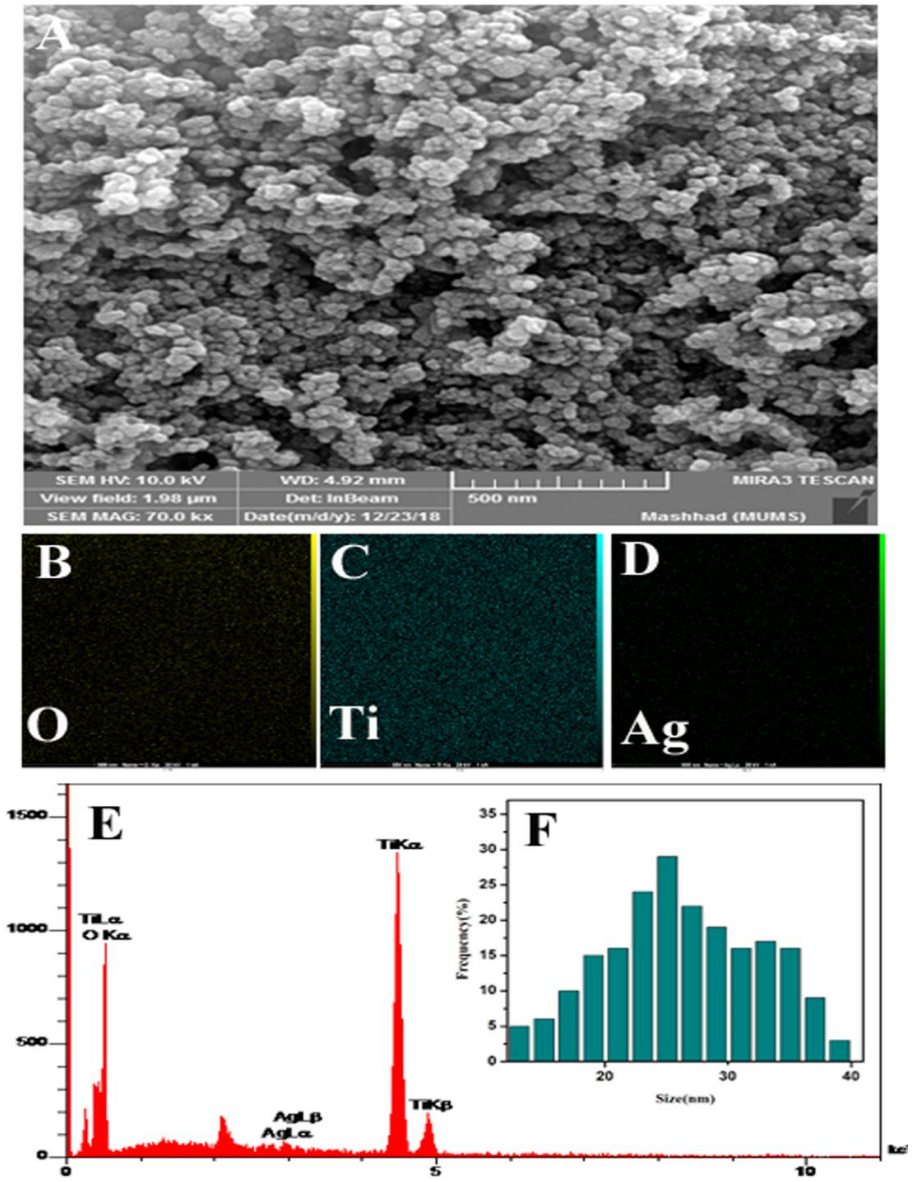

Fig. 4. SEM-EDS analysis results of Ag/TiO_2 NPs: (A) SEM image (B)–(D) EDS mapping result from (A) a SEM image showing the distribution of (B) O, (C) Ti and (D) Ag in a mass of Ag/TiO_2 NPs. (E) EDS spectrum (F) the corresponding particle size distributions.

an efficient route to alter anatase-to-rutile (A-R) phase transformation of nanosized Titania. Both doped samples exhibit broadening compared to pure TiO_2, which indicates the formation of smaller nanoparticles. The doping of Ag and Au is believed to form defects at the grain boundary, and then increase the potential energy for atomic diffusion. Thus, the transition from the anatase to the rutile phase was slightly suppressed by doping of TiO_2 [45].

Chemical structure

The FT-IR spectrum of synthesized TiO_2, 1%Au/TiO_2 and 1%Ag/TiO_2 nanoparticles is apparent in Fig. 1B. The peaks at 3350–3450 cm^{-1} and 1620–1635 are assigned to the stretching vibration of the O–H bond and bending vibration of adsorbed water molecules, respectively. FT-IR spectrum shows a broad intense peak below 1200 cm^{-1} due to Ti–O–Ti vibration and several peaks at 436–495 cm^{-1} and 550–653 cm^{-1} due to the absorption bands of O–Ti–O and Ti–O flexion vibration, respectively.

Morphological and elemental analysis

Figs. 2, 3 and 4 show the SEM-EDS pattern of synthesized TiO_2, Au/TiO_2 and Ag/TiO_2 nanoparticles, respectively. As is shown, the synthesized nanoparticles are global, uniform and slightly agglomerated. Furthermore, these figures show the corresponding particle size distributions as measured from SEM micrographs. It is observed that adding silver and gold reduces the particle size of TiO_2 nanoparticles which confirms the XRD results. The EDX data of TiO_2 nanoparticles shows several peaks around 0.2 and 4.5 keV. The intense peak is assigned to the bulk TiO_2 and the less intense one to the surface TiO_2. The peaks at 2.2 and 2.9 keV clearly confirmed the presence of gold and silver in the synthesized Au/TiO_2 and Ag/TiO_2 nanoparticles, respectively. In addition, to investigate the uniformity of the Au and Ag distribution, an elemental mapping analysis was conducted with EDS. From the mapping analysis results, Au and Ag were detected at nearly the same region where Ti is located in nanoparticles without segregation. On the other hand, bare TiO_2 nanoparticles showed no Au and Ag content.

Biological results

The neurotoxic activity of TiO_2, Au/TiO_2, and Ag/TiO_2 NPs was examined using the dose-dependent MTT assay (24 h). PC12 cells were exposed to treatment with various NPs at a concentration range of 5-100 µg/ml, followed by assessing the obtained cytotoxic activity. As shown in the charts (Fig. 5) for the impacts of various treatments on the survivability of PC12 cells, a concentration of 100 µg/ml from TiO_2, Au/TiO_2, and Ag/TiO_2 NPs significantly exerted cytotoxic activity as opposed to the control and the rest of groups ($P < 0.01$).

The morphology of PC12 cells was observed to study differentiation. To measure morphologically differentiated characteristics at the single-cell level, the efficiency of free NGF was first practiced as a differentiating factor. The treatment of PC12 cells with free NGF (Fig. 6,) leads to neurite outgrowth and forms a complex neural network. Nevertheless, an increase in neurite outgrowth was observed using NGF with TiO_2 NPs between 1 and 5 days after the induced differentiation (exactly neurite length). The treatment with NPs led to a significant effect on neurite length. The impacts of other NPs on neural differentiation were examined by incubating PC12 cells with combined NGF and NPs (Au/TiO_2 and Ag/TiO_2). Adding these NPs to the cells elevated the fraction of PC12 cells with longer neurites. According to the result, the addition of NPs raised both the percentage of neurites that originated from the soma and branching points of the cells.

The outcomes revealed that PC12 cells treated with NGF and Ag/TiO_2 NPs apparently enhanced considerably the neurite lengths and branching points as opposed to the other treatments, resulting in more complicated branching trees [Fig. 7 (a, b)]. Fig. 7 displays the dark blue appearance of Nissl substance (rough endoplasmic reticulum) because of the stained ribosomal RNA. Using the immunocytochemical assay, the neuron was visualized with anti-b3-tubulin, a neural-specific marker (Fig. 8). The exposure of PC12 cells to Ag/TiO_2 NPs led to the expression of neural marker protein.

According to our obtained data, the differentiation of PC12 cells can be induced by various kinds of TiO_2 NPs. In comparison to NPs incubated with free NGF, treatments with TiO_2, Au/TiO_2, and Ag/TiO_2 NPs elevated the effectiveness of NGF in the experiential situations of this study. In our research, it is noteworthy to address an essential subject, that is, various TiO_2 NPs significantly affected the neurite length and branching point. It is necessary to completely

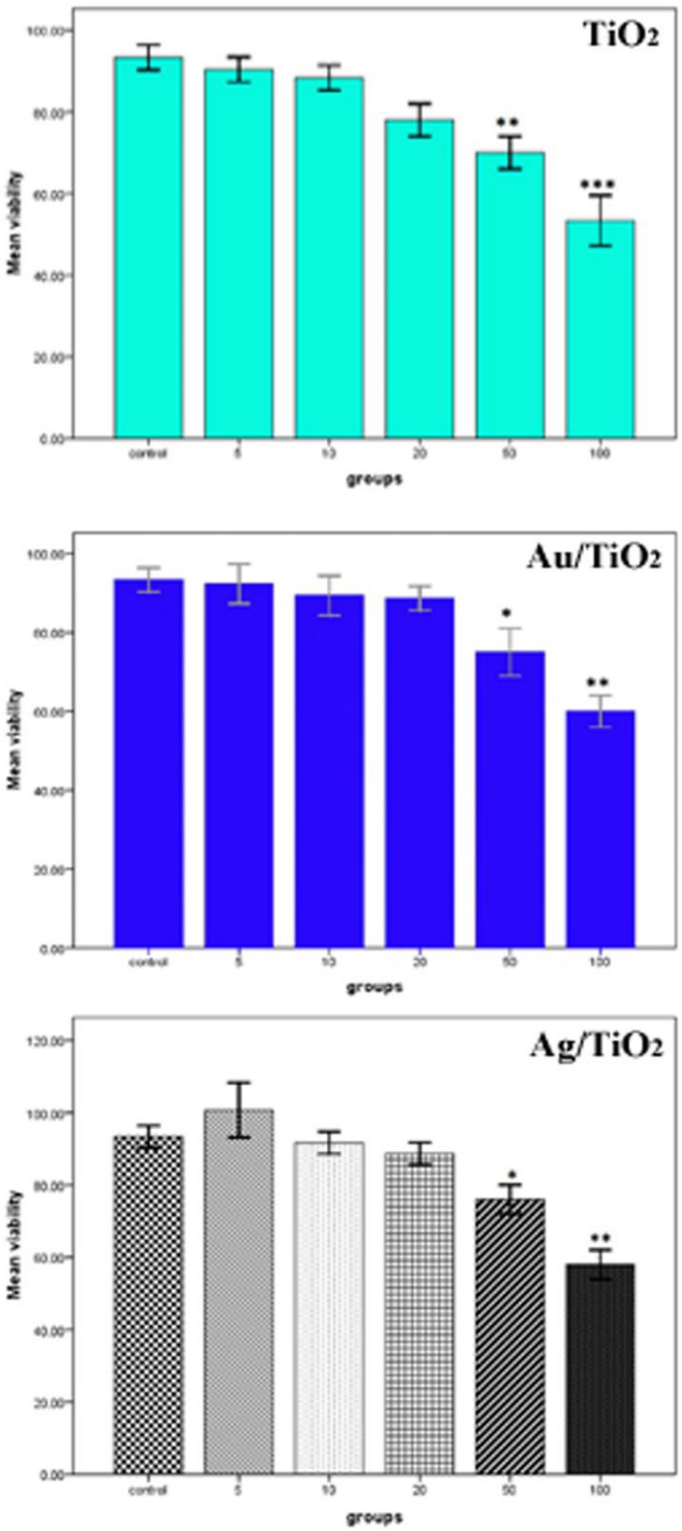

Fig. 5. Effect of different treatments on the viability of PC12 cells. There were significant differences between the viability of PC12 cells from different treatments (P<0.05). [* for P<0.05, ** for P<0.01 and *** for P<0.001].

understand the modes of action and meticulous routes of the communication between NPs and stem cells to fully exploit nanomaterials in treatments using stem cells. In stem cell culture systems, NPs are applied through a variety of techniques, including coating culture dishes, adding directly to the culture media, and conjunction of nanomaterials with a defined platform for 3D culture. The signaling of various growth factors is regulated by cell adhesion in neurons and neural cell lines (e.g., PC12 cells). Anchoring of cells is a significant stage in apoptosis, cell cycle regulation, and differentiation. The ligands of GFs (e.g., NGF) cause their optimal activation merely when cell adhesion is appropriate. Many reports demonstrate the interplay of NPs with intracellular constituents or cell membranes [46, 47]. The likely modes of action for the cellular internalization of NPs include clathrin and caveolin-dependent endocytosis, pinocytosis phagocytosis, and micropinocytosis [34, 47, 48]. Clathrin or caveolin-dependent endocytosis is supposedly the major

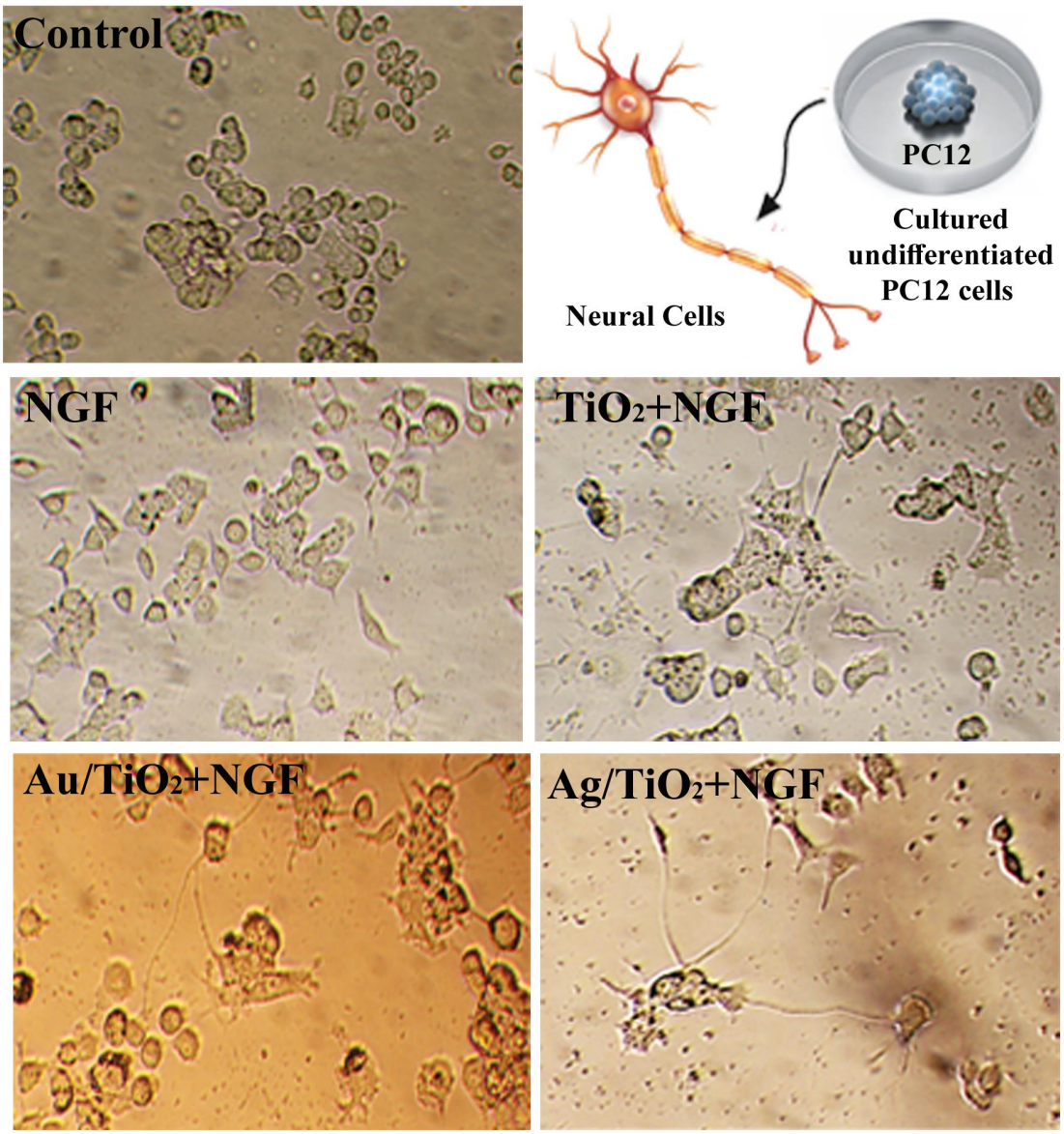

Fig. 6. Compartment between different treatment effects on neurite outgrowth. For each treatment, 100 cells in each of the three separate fields were counted.

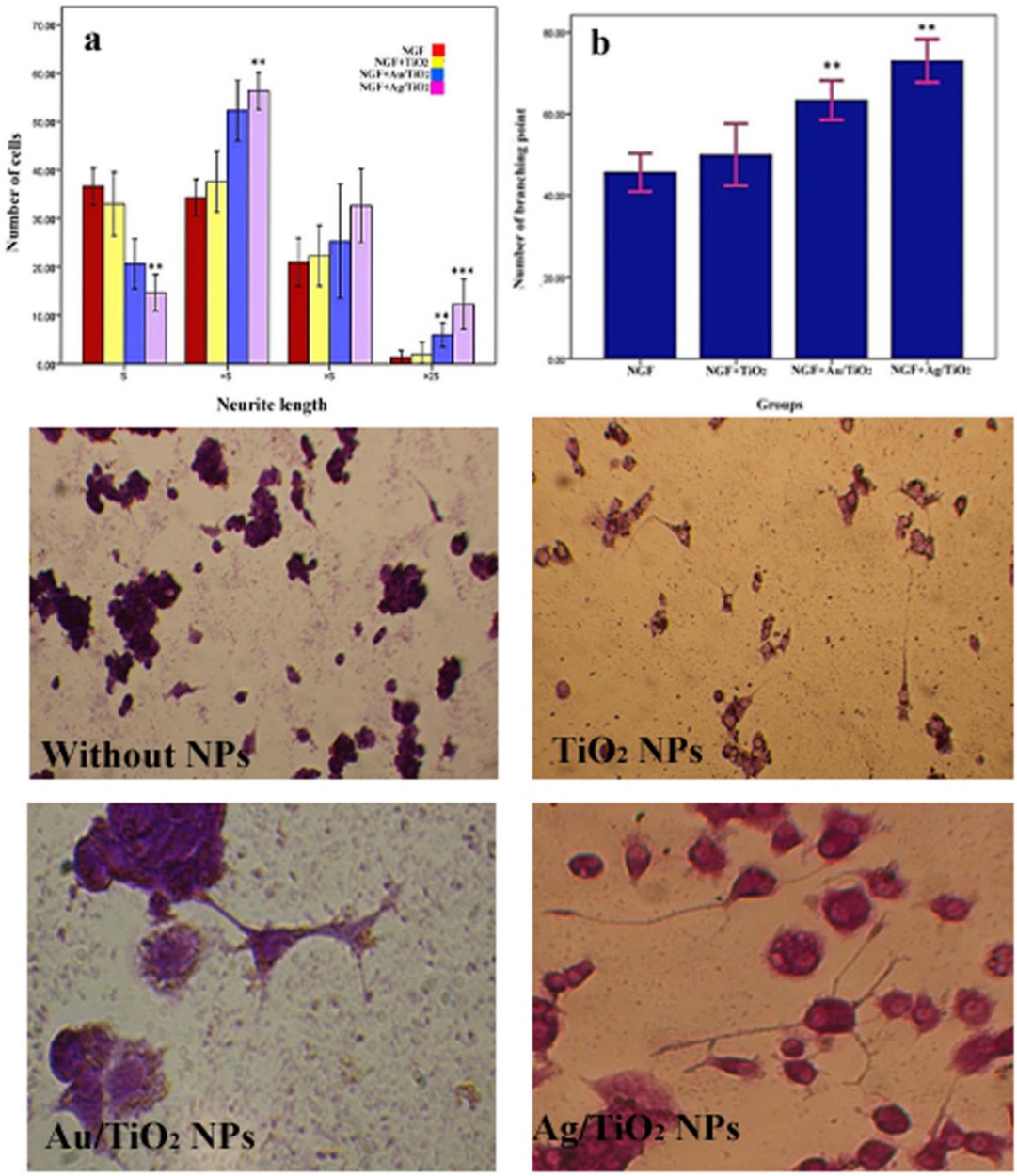

Fig. 7. Cresyl Violet Staining: the Nissl substance (rough endoplasmic reticulum) appeared dark blue due to the staining of ribosomal RNA. Distribution of the neurite of PC12 cells 5 day after the induction of differentiation (a - b).

mode of action for the intake of nanomaterials [49, 50]. NPs undergo exocytosis or are released through vesicle-dependent release, non-vesicle-dependent release, and lysosomal secretion. The magnitude of toxic activity can be determined by cellular retention and release of particles. The observation and quantification of the content of intracellular TiO_2 NPs in PC12 cells are possible by Prussian blue staining. As indicated by the MTT assay data, the cytotoxic activity of Ag/TiO_2 NPs is low at low concentrations. TiO_2 at high doses reportedly acts as a neurotoxin causing malfunction. A report by Sayes et al. also indicates that the growth rates of cells grown in

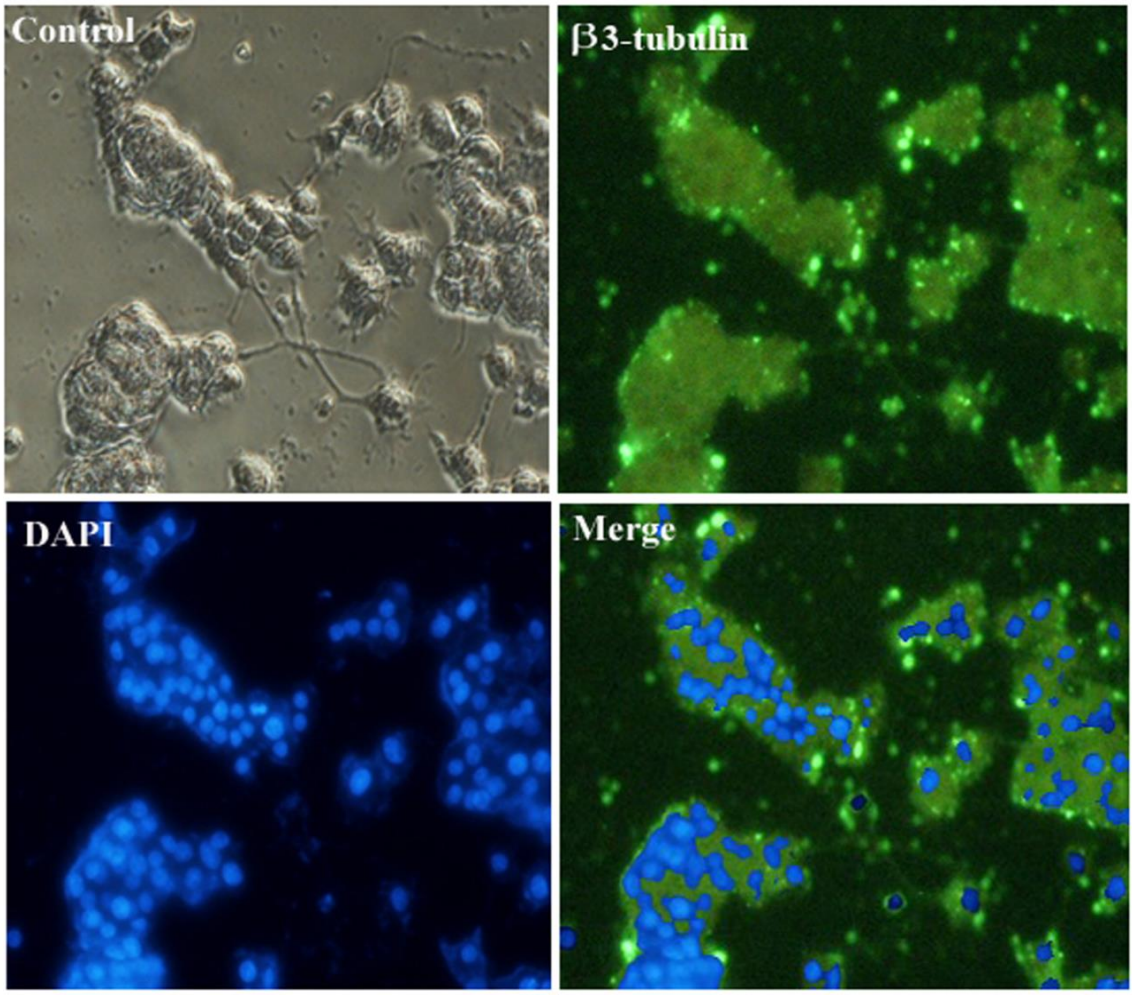

Fig. 8. Immunofluorescence images of differentiated PC12 cells 5 days after treatment with Ag/TiO_2 NPs. Green and blue fluorescence represent β3-tubulin and nucleus, respectively. Nuclei marked with DAPI. The fluorescent images were acquired using a fluorescence microscopy at a single focal plane.

association with TiO_2 NPs decline dramatically at concentrations > 100 mg/mL [51, 52].

To internalize NPs into the cells, important factors include the shape, size, and stiffness specifications of the surface and the hydrophobicity or hydrophilicity NPs [53]. For instance, there is an inverse correlation between the intake of NPs and particle size. Alternatively, evidence shows a greater intake of small-sized NPs (30–50 nm) than large-sized ones (50–200 nm), showing lower cellular internalization [54, 55]. Our synthesized TiO_2, Au/TiO_2, and Ag/TiO_2 NPs ranged from 23 to 29 nm in size, with a globular form, homogeneous, and slight agglomeration. Moreover, a greater intake rate was observed for globular NPs than that of non-globular ones [56]. In comparison to globular NPs with high internalization, cellular intake is lower in 2-D discoid NPs with high potentiality in binding to the cell surface [57]. Thus, the biological activity and toxicity of these particles are influenced by the shape, particle size, crystalline structure, and physicochemical features of NPs. Based on our observation, biomolecules on the anatase TiO_2 NPs were immobilized more efficiently than on rutile TiO_2 NPs. The Brunauer–Emmett–Teller (BET) analysis ascertained that the total pore volume was 4.2 times more in the anatase-type nanoparticle than that of the rutile form. The surface density of the hydroxyl group is higher in

the anatase phase of TiO_2 NPs, capable of clarifying charge carriers and stabilizing the biomolecules, thus lowering the recombination rate of electron–hole pairs [58]. The present data reveal that it is possible to precisely index the crystalline peaks of samples to the tetragonal anatase structured TiO_2. Additionally, good crystallinity in the synthesized TiO_2 NPs is represented by the sharp diffraction peaks, and the spectra represent no peaks for rutile and brookite structures. The physically and chemically modified nanoparticle surface via raising the hydrophobic property and softness reportedly results in an elevated internalization rate [59]. Notably, the surface charge of NPs is associated with cellular internalization rates. To modulate cellular events for a specific application in biomedicine, one of the recent tools is to prepare engineered NPs with the functional group of interest [60, 61]. The functionalization of TiO_2 nanorods with various functional groups, including poly (ethylene glycol) (–PEG), carboxyl groups (–COOH), and amines ($–NH_2$), led to their varied intake by rat bone marrow-derived MSCs (rBM-MSCs) (43).

The exclusive specifications, antimicrobial capability, biocompatible property, and low toxic activity have introduced Au and Ag NPs as promising substances to direct the fate of stem cells and tissue renewal. The current study concentrated on designing and preparing three types of TiO_2 NPs, i.e., a pure TiO_2 NP, and the other two types Au/TiO_2 and Ag/TiO_2 NPs. As an essential subject in this research, the joint application of Ag and TiO_2 NPs significantly elevated the neurite length and branching point.

CONCLUSION

To summarize, Findings of the present study showed that the combination of NGF with different TiO_2 nanoparticles is an effective method to increase the efficiency of differentiation. This treatment can be a suitable candidate for enhancing the efficiency of NGF during differentiation. The most important advantages of this method are the reduction of the oxidative stress that leads to maintaining the survival of PC12 cells, and induction of differentiation at excellent levels.

ACKNOWLEDGMENTS

Authors are grateful to the University of Kashan and the Iranian Nanotechnology Initiative Council for providing financial support to undertake this work.

CONFLICT OF INTEREST

The authors declare that there is no conflict of interests regarding the publication of this manuscript.

REFERENCES

1. Ramalingam V, Sundaramahalingam S, Rajaram R. Size-dependent antimycobacterial activity of titanium oxide nanoparticles against Mycobacterium tuberculosis. Journal of Materials Chemistry B. 2019;7(27):4338-4346.
2. Sun W, Dong X, Huang P, Shan J, Qi L, Zhou J. Solvothermal synthesis of Nb-doped TiO_2 nanoparticles with enhanced sonodynamic effects for destroying tumors. RSC Advances. 2021;11(58):36920-36927.
3. Fei Yin Z, Wu L, Gui Yang H, Hua Su Y. Recent progress in biomedical applications of titanium dioxide. Physical Chemistry Chemical Physics. 2013;15(14):4844.
4. Zhang J, Cai X, Zhang Y, Li X, Li W, Tian Y, et al. Imaging cellular uptake and intracellular distribution of TiO2 nanoparticles. Analytical Methods. 2013;5(23):6611.
5. Gage FH. Mammalian Neural Stem Cells. Science. 2000;287(5457):1433-1438.
6. Kalyani A, Hobson K, Rao MS. Neuroepithelial Stem Cells from the Embryonic Spinal Cord: Isolation, Characterization, and Clonal Analysis. Dev Biol. 1997;186(2):202-223.
7. Honda S, Nakajima K, Nakamura Y, Imai Y, Kohsaka S. Rat primary cultured microglia express glial cell line-derived neurotrophic factor receptors. Neurosci Lett. 1999;275(3):203-206.
8. Temple S. The development of neural stem cells. Nature. 2001;414(6859):112-117.
9. Hackelberg S, Tuck SJ, He L, Rastogi A, White C, Liu L, et al. Nanofibrous scaffolds for the guidance of stem cell-derived neurons for auditory nerve regeneration. PLoS One. 2017;12(7):e0180427.
10. Haddad T, Noel S, Liberelle B, El Ayoubi R, Ajji A, De Crescenzo G. Fabrication and surface modification of poly lactic acid (PLA) scaffolds with epidermal growth factor for neural tissue engineering. Biomatter. 2016;6(1):e1231276.
11. Huang D, Lin C, Wen X, Gu S, Zhao P. A Potential Nanofiber Membrane Device for Filling Surgical Residual Cavity to Prevent Glioma Recurrence and Improve Local Neural Tissue Reconstruction. PLoS One. 2016;11(8):e0161435.
12. Chowdhury EH. Nanotherapeutics: CRC Press; 2016 2016/04/21.
13. Bhang SH, Han J, Jang H-K, Noh M-K, La W-G, Yi M, et al. pH-triggered release of manganese from MnAu nanoparticles that enables cellular neuronal differentiation without cellular toxicity. Biomaterials. 2015;55:33-43.
14. Wang K, He X, Linthicum W, Mezan R, Wang L, Rojanasakul Y, et al. Carbon nanotubes induced fibrogenesis on nanostructured substrates. Environ Sci: Nano. 2017;4(3):689-699.
15. Selective Targeting of Neurons with Inorganic Nanoparticles: Revealing the Crucial Role of Nanoparticle Surface Charge. American Chemical Society (ACS).
16. Guerzoni LPB, Nicolas V, Angelova A. In Vitro Modulation

of TrkB Receptor Signaling upon Sequential Delivery of Curcumin-DHA Loaded Carriers Towards Promoting Neuronal Survival. Pharm Res. 2016;34(2):492-505.
17. Sun B, Taing A, Liu H, Nie G, Wang J, Fang Y, et al. Nerve Growth Factor-Conjugated Mesoporous Silica Nanoparticles Promote Neuron-Like PC12 Cell Proliferation and Neurite Growth. Journal of Nanoscience and Nanotechnology. 2016;16(3):2390-2393.
18. Murphy CJ, Jana NR. Controlling the Aspect Ratio of Inorganic Nanorods and Nanowires. Adv Mater. 2002;14(1):80-82.
19. Franca E, Jao PF, Fang S-P, Alagapan S, Pan L, Yoon JH, et al. Scale of Carbon Nanomaterials Affects Neural Outgrowth and Adhesion. IEEE Trans NanoBiosci. 2016;15(1):11-18.
20. Swapnil Suman SSea, et al. Experimental Investigation on Influence of Functionalized Multi-Walled Carbon Nanotubes on Surface Roughness in Drilling of CFRP Composites. International Journal of Mechanical and Production Engineering Research and Development. 2018;8(3):1133-1146.
21. Singh N, Chen J, Koziol KK, Hallam KR, Janas D, Patil AJ, et al. Chitin and carbon nanotube composites as biocompatible scaffolds for neuron growth. Nanoscale. 2016;8(15):8288-8299.
22. Singh A, Kim W, Kim Y, Jeong K, Kang CS, Kim Y, et al. Theranostics: Multifunctional Photonics Nanoparticles for Crossing the Blood–Brain Barrier and Effecting Optically Trackable Brain Theranostics (Adv. Funct. Mater. 39/2016). Adv Funct Mater. 2016;26(39):7025-7025.
23. Gholamine B, Karimi I, Salimi A, Mazdarani P, Becker LA. Neurobehavioral toxicity of carbon nanotubes in mice. Toxicology and Industrial Health. 2016;33(4):340-350.
24. Wei M, Li S, Yang Z, Zheng W, Le W. Gold nanoparticles enhance the differentiation of embryonic stem cells into dopaminergic neurons via mTOR/p70S6K pathway. Nanomedicine. 2017;12(11):1305-1317.
25. Hsiao IL, Chang C-C, Wu C-Y, Hsieh Y-K, Chuang C-Y, Wang C-F, et al. Indirect effects of TiO2 nanoparticle on neuron-glial cell interactions. Chemico-Biological Interactions. 2016;254:34-44.
26. Lin R, Li Y, MacDonald T, Wu H, Provenzale J, Peng X, et al. Improving sensitivity and specificity of capturing and detecting targeted cancer cells with anti-biofouling polymer coated magnetic iron oxide nanoparticles. Colloids Surf B Biointerfaces. 2017;150:261-270.
27. El-Sayed MA. Some Interesting Properties of Metals Confined in Time and Nanometer Space of Different Shapes. Acc Chem Res. 2001;34(4):257-264.
28. Dos Santos Ramos MA, Da Silva P, Spósito L, De Toledo L, Bonifácio B, Rodero CF, et al. Nanotechnology-based drug delivery systems for control of microbial biofilms: a review. International Journal of Nanomedicine. 2018;Volume 13:1179-1213.
29. Melo Jr MA, Santos LSS, Gonçalves MdC, Nogueira AF. Preparação de nanopartículas de prata e ouro: um método simples para a introdução da nanociência em laboratório de ensino. Quim Nova. 2012;35(9):1872-1878.
30. Abdal Dayem A, Lee S, Cho S-G. The Impact of Metallic Nanoparticles on Stem Cell Proliferation and Differentiation. Nanomaterials. 2018;8(10):761.
31. Bao H, Cheng S, Li X, Li Y, Yu C, Huang J, et al. Functional Au nanoparticles for engineering and long-term CT imaging tracking of mesenchymal stem cells in idiopathic pulmonary fibrosis treatment. Biomaterials. 2022;288:121731.
32. Samberg ME, Loboa EG, Oldenburg SJ, Monteiro-Riviere NA. Silver nanoparticles do not influence stem cell differentiation but cause minimal toxicity. Nanomedicine. 2012;7(8):1197-1209.
33. He W, Kienzle A, Liu X, Müller WEG, Elkhooly TA, Feng Q. In Vitro; Effect of 30 nm Silver Nanoparticles on Adipogenic Differentiation of Human Mesenchymal Stem Cells. J Biomed Nanotechnol. 2016;12(3):525-535.
34. Bannunah AM, Vllasaliu D, Lord J, Stolnik S. Mechanisms of Nanoparticle Internalization and Transport Across an Intestinal Epithelial Cell Model: Effect of Size and Surface Charge. Mol Pharm. 2014;11(12):4363-4373.
35. Chang K-B, Shen C-C, Hsu S-h, Tang CM, Yang Y-C, Liu S-Y, et al. Corrigendum to Functionalized collagen-silver nanocomposites for evaluation of the biocompatibility and vascular differentiation capacity of mesenchymal stem cells Volume 624 (2021), 126814. Colloids Surf Physicochem Eng Aspects. 2022;648:129372.
36. Ahmadi S, Pilehvar Y, Zarghami N, Abri A. Efficient osteoblastic differentiation of human adipose-derived stem cells on TiO_2 nanoparticles and metformin co-embedded electrospun composite nanofibers. J Drug Deliv Sci Technol. 2021;66:102798.
37. Tian J, Zhao Z, Kumar A, Boughton RI, Liu H. Recent progress in design, synthesis, and applications of one-dimensional TiO_2 nanostructured surface heterostructures: a review. Chem Soc Rev. 2014;43(20):6920-6937.
38. Franco M, Viscione A, Rigo L, Guidi R, Brunelli G, Avantaggiato A, et al. Osseotite implants inserted into fresh frozen bone grafts. J Maxillofac Oral Surg. 2009;8(3):201-204.
39. Gapski R, Wang H-L, Mascarenhas P, Lang NP. Critical review of immediate implant loading. Clin Oral Implants Res. 2003;14(5):515-527.
40. Liu X, Ren X, Deng X, Huo Y, Xie J, Huang H, et al. A protein interaction network for the analysis of the neuronal differentiation of neural stem cells in response to titanium dioxide nanoparticles. Biomaterials. 2010;31(11):3063-3070.
41. Park J, Bauer S, Schlegel KA, Neukam FW, von der Mark K, Schmuki P. TiO_2 Nanotube Surfaces: 15 nm—An Optimal Length Scale of Surface Topography for Cell Adhesion and Differentiation. Small. 2009;5(6):666-671.
42. Kommireddy DS, Sriram SM, Lvov YM, Mills DK. Stem cell attachment to layer-by-layer assembled TiO_2 nanoparticle thin films. Biomaterials. 2006;27(24):4296-4303.
43. Shrestha S, Mao Z, Fedutik Y, Gao C. Influence of titanium dioxide nanorods with different surface chemistry on the differentiation of rat bone marrow mesenchymal stem cells. Journal of Materials Chemistry B. 2016;4(43):6955-6966.
44. Vercellino M, Ceccarelli G, Cristofaro F, Balli M, Bertoglio F, Bruni G, et al. Nanostructured TiO_2 Surfaces Promote Human Bone Marrow Mesenchymal Stem Cells Differentiation to Osteoblasts. Nanomaterials. 2016;6(7):124.
45. Zhang Y, Zhang H, Xu Y, Wang Y. Significant effect of lanthanide doping on the texture and properties of nanocrystalline mesoporous TiO_2. J Solid State Chem. 2004;177(10):3490-3498.
46. Mocan L, Ilie, Mocan T. Influence of nanomaterials on stem cell differentiation: designing an appropriate nanobiointerface. International Journal of Nanomedicine. 2012:2211.

47. Park JH, Oh N. Endocytosis and exocytosis of nanoparticles in mammalian cells. International Journal of Nanomedicine. 2014:51.
48. Yameen B, Choi WI, Vilos C, Swami A, Shi J, Farokhzad OC. Insight into nanoparticle cellular uptake and intracellular targeting. Journal of Controlled Release. 2014;190:485-499.
49. Wang Z, Tiruppathi C, Minshall RD, Malik AB. Size and Dynamics of Caveolae Studied Using Nanoparticles in Living Endothelial Cells. ACS Nano. 2009;3(12):4110-4116.
50. Pelkmans L, Kartenbeck J, Helenius A. Caveolar endocytosis of simian virus 40 reveals a new two-step vesicular-transport pathway to the ER. Nat Cell Biol. 2001;3(5):473-483.
51. Sayes CM, Wahi R, Kurian PA, Liu Y, West JL, Ausman KD, et al. Correlating Nanoscale Titania Structure with Toxicity: A Cytotoxicity and Inflammatory Response Study with Human Dermal Fibroblasts and Human Lung Epithelial Cells. Toxicol Sci. 2006;92(1):174-185.
52. Gurr J-R, Wang ASS, Chen C-H, Jan K-Y. Ultrafine titanium dioxide particles in the absence of photoactivation can induce oxidative damage to human bronchial epithelial cells. Toxicology. 2005;213(1-2):66-73.
53. Kerativitayanan P, Carrow JK, Gaharwar AK. Nanomaterials for Engineering Stem Cell Responses. Advanced Healthcare Materials. 2015;4(11):1600-1627.
54. Li J, Li JEJ, Zhang J, Wang X, Kawazoe N, Chen G. Gold nanoparticle size and shape influence on osteogenesis of mesenchymal stem cells. Nanoscale. 2016;8(15):7992-8007.
55. Ko W-K, Heo DN, Moon H-J, Lee SJ, Bae MS, Lee JB, et al. The effect of gold nanoparticle size on osteogenic differentiation of adipose-derived stem cells. Journal of Colloid and Interface Science. 2015;438:68-76.
56. Florez L, Herrmann C, Cramer JM, Hauser CP, Koynov K, Landfester K, et al. How Shape Influences Uptake: Interactions of Anisotropic Polymer Nanoparticles and Human Mesenchymal Stem Cells. Small. 2012;8(14):2222-2230.
57. Zhang S, Gao H, Bao G. Physical Principles of Nanoparticle Cellular Endocytosis. ACS Nano. 2015;9(9):8655-8671.
58. Zhang Z, Xie Y, Liu Z, Rong F, Wang Y, Fu D. Covalently immobilized biosensor based on gold nanoparticles modified TiO_2 nanotube arrays. J Electroanal Chem. 2011;650(2):241-247.
59. Lorenz S, Hauser CP, Autenrieth B, Weiss CK, Landfester K, Mailänder V. The Softer and More Hydrophobic the Better: Influence of the Side Chain of Polymethacrylate Nanoparticles for Cellular Uptake. Macromol Biosci. 2010;10(9):1034-1042.
60. Tekin H, Sanchez JG, Landeros C, Dubbin K, Langer R, Khademhosseini A. Controlling Spatial Organization of Multiple Cell Types in Defined 3D Geometries. Adv Mater. 2012;24(41):5543-5547.
61. Zorlutuna P, Annabi N, Camci-Unal G, Nikkhah M, Cha JM, Nichol JW, et al. Microfabricated Biomaterials for Engineering 3D Tissues. Adv Mater. 2012;24(14):1782-1804.